



## Obrabotka metallov - Metal Working and Material Science

Journal homepage: [http://journals.nstu.ru/obrabotka\\_metallov](http://journals.nstu.ru/obrabotka_metallov)



### Determination of the optimal metal processing mode when analyzing the dynamics of cutting control systems

Victor Lapshin<sup>a, \*</sup>, Denis Moiseev<sup>b</sup>

Don State Technical University, 1 Gagarin square, Rostov-on-Don, 344000, Russian Federation

<sup>a</sup>  <https://orcid.org/0000-0002-5114-0316>,  [lapshin1917@yandex.ru](mailto:lapshin1917@yandex.ru); <sup>b</sup>  <https://orcid.org/0000-0002-7186-7758>,  [denisey2003@mail.ru](mailto:denisey2003@mail.ru)

#### ARTICLE INFO

##### Article history:

Received: 15 December 2022

Revised: 12 January 2023

Accepted: 21 January 2023

Available online: 15 March 2023

##### Keywords:

Dynamics  
Tool vibration  
Cutting stability  
Processing speed  
Wear and tear  
Regenerative effect

##### Acknowledgements

Research were partially conducted at core facility “Structure, mechanical and physical properties of materials”.

#### ABSTRACT

**Introduction.** In numerous experimental studies of metal cutting processes on metal-cutting equipment, the existence of some optimal processing mode is noted, which was most vividly formulated by *A.D. Makarov* in his point on the existence of an optimal cutting temperature (processing speed). Here, by the authors from Russia, the emphasis is on the description of the optimality of cutting processes related to the properties of the processed material and the properties of the tool used in this process. However, there is another opinion in the Western scientific literature, which is generally based on the regenerative nature of vibrations in cutting dynamics. Vibration regeneration is associated with the dynamics of the cutting process, which is significantly affected by a lagging argument reflecting the variability of the cut layer. The connection of these two approaches is seen through the analysis of the stability domain of the dynamic cutting system in the parameter space: cutting speeds and tool wear values. **Subject.** Based on this, the paper considers the question of the relationship between the optimal according to *A.D. Makarov* the processing mode and the dynamics of the cutting process, including the regeneration of tool vibrations during metal turning. To do this, two research hypotheses are formulated and numerical modeling is performed in order to determine its reliability. **Purpose of the work:** to consider the position of *A.D. Makarov* on the existence of an optimal cutting mode, from the point of view of the stability of the dynamics of metal turning. For this purpose, two hypotheses are put forward in the work to be analyzed. **The paper investigates:** a mathematical model describing the dynamics of vibration oscillations of the cutting wedge tip, taking into account the dynamics of the temperature formed in the contact zone and its influence on the forces that prevent the forming motions of the tool. **Research methods:** a series of field experiments was carried out on a metalworking equipment using the capabilities of the measuring stand *STD.201-1*, the purpose of which was to determine the effect of the thermal expansion of metals on the value of the buoyant force. Based on numerical simulation of the initial nonlinear mathematical models, as well as simulation of models linearized in the vicinity of the equilibrium point, an analysis of the stability of the cutting system with variations in the cutting speed and the amount of tool wear along the flank is conducted. **The results of the work.** The results of field experiments are presented, which showed a significant linear increase in the force pushing out the tool with an increase in temperature in the contact zone of the tool and the workpiece. The results of simulation of the state and the corresponding phase trajectories when the cutting wedge is embedded in the workpiece, as well as the forces decomposed along the axis of deformation of the tool, are presented. The results of modeling the *Mikhailov* vector hodograph for a linearized model of the dynamics of the cutting process are presented. **Conclusions:** The research results have shown that only the second hypothesis put forward by the authors makes it possible to adequately interpret the point put forward by *A.D. Makarov*. The main addition to the description of the point of *A.D. Makarov*, the authors consider it necessary to take into account changes in the pushing force with an increase in the temperature of the contact zone of the tool and the workpiece.

**For citation:** Lapshin V.P., Moiseev D.V. Determination of the optimal metal processing mode when analyzing the dynamics of cutting control systems. *Obrabotka metallov (tehnologiya, oborudovanie, instrumenty) = Metal Working and Material Science*, 2023, vol. 25, no. 1, pp. 16–43. DOI: 10.17212/1994-6309-2023-25.1-16-43. (In Russian).

#### \* Corresponding author

Lapshin Viktor P., Ph.D. (Engineering), Associate Professor  
Don State Technical University,  
1 Gagarin square  
344000, Rostov-on-don, Russian Federation  
Tel.: 8 (900) 122-75-14, e-mail: [lapshin1917@yandex.ru](mailto:lapshin1917@yandex.ru)

## Introduction

The quality of machining, as well as the cutter power, is associated with the stability of the vibration dynamics of the cutting process. Vibrations of the tool tip during cutting depend on two groups of factors, the first group is vibration activity unrelated to processes occurring in the cutting zone, and the second group is vibration activity caused by processes occurring in the cutting zone. In this regard, the development of technologies and methods for minimizing vibration activity, the nature of which is determined by the cutting process, is of great importance.

The vibrations of the tool accompanying the cutting process are largely determined by the regeneration of vibrations when cutting along the “*trace*”, which is called the *regenerative effect* [1–4]. In these papers, it is noted that the main factor influencing the regenerative effect is the so-called “*time delay*” [5–7], it determines the stability of the process dynamics. In addition to the regenerative nature of the self-excitation vibration dynamics of the cutting system, the stability of the cutting tool vibrations is affected by: the temperature in the contact zone of the tool and the workpiece [8]; changes in the force response from the cutting process to the forming motions of the tool [9]; the value characterizing the degree of the cutting wedge wear, etc. [10]. However, the developing synergetic concept describing the processes occurring in machines [11–12] allows us to speak not about every individual factor, but about a certain set of interrelated and interacting factors that determine the mechanism of self-excitation of the cutting control system [13–14].

The most important factor in the complexity of the mathematical description of cutting processes dynamics is, already mentioned earlier, the “*time delay*”, which determines the regenerative nature of the self-excitation of the cutting system. It should be noted that in the process of linearization of a system of integro-differential equations describing the complex, nonlinear, delayed dynamics of the cutting process, one will have to deal with an element containing a lagging argument. Such an element will not allow an analysis of cutting control system differential equations using a linearized model in the vicinity of the equilibrium point based on algebraic criteria, such as *Hurwitz* criterion [15], or *Raus* criterion [16]. The solution to this problem is the use of frequency stability criteria, such as the *Nyquist* criterion [17–18], or its Soviet counterpart, the *Mikhailov* criterion [19–21]. The *Nyquist* criterion itself, applied to mathematical models of metal cutting control systems, is well considered in research papers of V.L. *Zakorotny* [11, 12], but *Mikhailov's* criterion, well-known and long-known in the American engineering school [21], is not widely used yet.

The purpose of such modeling is to determine some best cutting mode; such a mode, in which self-excitation factor of the cutting control system will be minimized. It has already been experimentally proved that such a mode exists, and it is related to the cutting speed [22, 23]. In these research papers, the best mode is understood as the mode that provides the minimum roughness of the processed surface and the maximum dimensional stability of the cutting tool. For example, A.D. *Makarov*, in his monograph [22], formulates the following statement: “*the most important factor determining the characteristics of the cutting process is the average contact temperature determined by the cutting mode (cutting speed).*” In this and other papers, the tool contact temperature is determined by the current power released during cutting and converted into heat, which linearly depends on the cutting speed. However, in the paper [8] it was shown that when the wear of the cutting wedge along the flank is formed, an additional thermodynamic feedback is formed, which pre-warms the cutting zone for the period up to the current moment of cutting. In the future, this will lead to a thermal expansion of the workpiece material, which will increase the value of the force pushing the tool. It should be noted that this factor, the restructuring of the force reaction, which is confirmed by experimental studies [9], was not previously taken into account when forming mathematical models of cutting systems.

A.D. *Makarov* himself, in his reasoning, relied on the following well-known factors:

- 1) the falling nature of the cutting force (temperature-speed factor of processing), identified and presented as a graphical characteristic in the works of N.N. *Zorev* [24];
- 2) the existence of “favorable conditions” in the cutting zone, interpreted by the transition from the adhesive nature to the diffusion nature of friction [22].



In the diagram shown in Figure 1, deformations are decomposed into three main axes:  $x$ -axis is the axial direction of deformations (mm),  $y$ -axis is the radial direction of deformations (mm) and  $z$ -axis is the tangential direction of deformations (mm). Along the same axes, the force response decomposes from the cutting process into the forming motions of the tool ( $F_f, F_p, F_c(N)$ ),  $V_f$  and  $V_c$  (mm/s) feed and cutting speeds, respectively,  $\omega$  is the angular velocity of the spindle (rev/s).

The description of the cutting force is generalized, based on the point of proportionality of its area of the cut layer, in the form:

$$F_i = \rho a_p S \chi_i, \quad (1)$$

where  $\chi_i$  – a certain expansion coefficient of the general vector of response forces on the  $i$ -axis of the tool deformation; it should be noted that this approach is widely used within the scientific school of *V.L. Zakorotny* [12], the depth of processing also depends on the deformations of the tool and the workpiece  $a_p = a_{p0} - y$ , where  $t_{p0}$  technologically specified processing depth without taking into account deformations of the tool and the workpiece, the amount of feed per revolution –  $S$ .

The feed value can be represented as the following integral:

$$S = \int_{t-T_V}^t \left( V_f - \frac{dx}{dt} \right) dt, \quad (2)$$

where  $T_V$  – revolution period of the workpiece.

The most important component of the cutting force is the force component, which is formed not in the zone of primary deformation and friction of the cuttings on the tool face, but on the tool flank, where the pushing force and friction force are formed in the direction of the primary motion. This component of the force depends on the wear of the tool along the flank, therefore, based on the approach proposed in the work of *V.L. Zakorotny* [22], we describe the force formed here as:

$$F_h = \sigma S_h e^{-K_h x}, \quad (3)$$

where  $\sigma$  – compressive strength of the processed metal in (kg/mm<sup>2</sup>);  $K_h$  – the coefficient of the increase steepness in force,  $S_h$  – the contact area of the tool and the workpiece along the flank of the cutting wedge, which is defined as:  $S_h = h_3 t_p$ ,  $K_h$  – the coefficient determining the steepness of the nonlinear increase in the contact area of the tool and the workpiece when the tool and the workpiece approach.

Through the side cutting edge angle –  $\varphi$ , we decompose the force reaction on the  $x$  and  $y$  axes of the formation, as follows:

$$\begin{cases} F_h^{(x)} = \cos \varphi F_h \\ F_h^{(y)} = \sin \varphi F_h \end{cases}. \quad (4)$$

The force response in the direction of  $z$  coordinate is, in essence, nothing more than the friction force, which can be represented as:

$$F_h^{(z)} = k_f F_h, \quad (5)$$

where  $k_f$  – coefficient of friction.

Using the approach proposed by *A.D. Makarov* [22], we identify the characteristic of friction coefficient by the following expression:

$$k_f = k_{0f} + \Delta k_f \left[ e^{-K_{f1} Q} + e^{K_{f2} Q} \right] / 2, \quad (6)$$

where  $k_{0f}$  – some constant minimum value of the friction coefficient,  $\Delta k_f$  – the value of the increment of the friction coefficient when the temperature changes in the contact zone,  $K_{f1}$  and  $K_{f2}$  – coefficients determining the steepness of the fall and growth characteristics of the friction coefficient.

Thus, generalizing the description of the force response from the cutting process to the forming motions of the tool, we obtain the following equations describing the force response:

$$\begin{cases} F_f = \chi_1 F + F_h^{(x)}, \\ F_p = \chi_2 F + F_h^{(y)}, \\ F_c = \chi_3 F + F_h^{(z)}. \end{cases} \quad (7)$$

In addition to the power and thermodynamic subsystems of the cutting system, in the general structure of the control system (see Figure 1), there is a subsystem of deformation motions of the tool tip, which was indirectly included in our reasoning, but is not directly represented by the model. Taking into account the dependencies of response forces proposed by Equation 6, as well as relying on the approach to modeling the dynamics of the deformation motion of the tool used in the scientific school of *V.L. Zakorotny* [12], we assume that the model of a tool tip deformations will take the following form:

$$\begin{cases} m \frac{d^2 x}{dt^2} + h_{11} \frac{dx}{dt} + h_{12} \frac{dy}{dt} + h_{13} \frac{dz}{dt} + c_{11}x + c_{12}y + c_{13}z = F_f, \\ m \frac{d^2 y}{dt^2} + h_{21} \frac{dx}{dt} + h_{22} \frac{dy}{dt} + h_{23} \frac{dz}{dt} + c_{21}x + c_{22}y + c_{23}z = F_p, \\ m \frac{d^2 z}{dt^2} + h_{31} \frac{dx}{dt} + h_{32} \frac{dy}{dt} + h_{33} \frac{dz}{dt} + c_{31}x + c_{32}y + c_{33}z = F_c. \end{cases} \quad (8)$$

where  $[kg \cdot s^2 / mm]$ ;  $h [kg \cdot s / mm]$ ;  $\tilde{n} [kg / mm]$  – matrices of inertia coefficients, dissipation coefficients and stiffness coefficients, respectively.

As a result of the cutting wedge evolution, a contact area is formed along the flank, the length of which determines the interaction time, as well as the interaction time is determined by the cutting speed. The conversion of cutting power to temperature requires a preliminary formalized description of the most instantaneous cutting power, which is conveniently represented by the following expression:

$$N = F_c \left( V_c - \frac{dz}{dt} \right) = \left( \chi_3 F + F_h^{(z)} \right) \left( V_c - \frac{dz}{dt} \right). \quad (9)$$

Using the approach proposed in [8], let's synthesize a differential equation describing the thermodynamic component of the system as:

$$T_1 T_2 \frac{d^2 Q_z}{dt^2} + (T_1 + T_2) \frac{dQ_z}{dt} + Q_z = kN, \quad (10)$$

where  $T_1 = \frac{\lambda}{\alpha_1}$ ,  $T_2 = \frac{T_h}{\alpha_2} = \frac{h_3}{V_c \alpha_2}$ ,  $k = \frac{k_Q \lambda h_3}{\alpha_1 \alpha_2 V_c}$  – transmission ratio,  $\alpha_1, \alpha_2$  – dimensionless scaling parameters,  $\lambda$  – the coefficient of thermal conductivity,  $k_Q$  – the coefficient characterizing the conversion of irreversible transformations power released in the tool/workpiece contact zone into temperature.

Thus, the system of equations (8)–(10) will be the mathematical model of the cutting system.

### *Mikhailov criterion and linearization of the system of equations*

To assess the stability of the control system based on the *Mikhailov* criterion, the characteristic polynomial of the transfer function of the control system is used:

$$D(p) = a_0 p^n + a_1 p^{n-1} + \dots + a_{n-1} p + a_n \quad (11)$$

where  $n$  – the degree of polynomial and it is also the order of the differential equation, for the case represented by the expression (8), (10),  $n = 8$ .

Assuming  $p = j\omega$ , we transform the characteristic polynomial into a complex frequency polynomial:

$$D(j\omega) = a_0(j\omega)^n + a_1(j\omega)^{n-1} + \dots + a_{n-1}(j\omega) + a_n.$$

In case of stable systems, the hodograph of the *Mikhailov* vector has the property of starting from the point  $U(0) = a_n$ ,  $V(0) = 0$ . As  $\omega$  increases from zero to infinity, the point  $M(U, V)$  moves to the left so that the curve tends to cover the origin, while moving away from it. If we draw the radius vector from the origin to the point  $M(U, V)$ , it turns out that the radius vector rotates counterclockwise, continuously increasing.

The *Mikhailov* criterion itself is formulated as follows: when the frequency changes from zero to infinity, the *Mikhailov* hodograph begins on the real axis at point  $a_n$ , sequentially passes counterclockwise  $n$  quadrants of the complex plane without passing through zero, and goes to infinity in the  $n^{\text{th}}$  quadrant, the system is stable. In case of unstable systems, the curves do not cover the origin, while if the hodograph starts from the origin or passes through the origin, the system is on the stability boundary.

To assess the stability of the control system by the *Mikhailov* method, it is necessary to determine the characteristic polynomial of the control system, described by the system of equations (8), (10). As this system is nonlinear, the first thing that is required is to linearize this system of equations in some vicinity of the equilibrium point, which is done below.

$$\left\{ \begin{aligned} & m \frac{d^2 x}{dt^2} + h_{11} \frac{dx}{dt} + h_{12} \frac{dy}{dt} + h_{13} \frac{dz}{dt} + x \left[ c_{11} + \chi_1 (1 - e^{-jT_v \omega}) (\rho + \rho \mu) + \cos(\varphi) h_3 \sigma t_p \alpha_2 \right] + \\ & + y \left[ c_{12} + \chi_1 (\rho + \rho \mu) S_p + \cos(\varphi) \sigma h_3 \right] + c_{13} z + Q \chi_1 \rho \mu \alpha_1 t_p S_p = 0, \\ & m \frac{d^2 y}{dt^2} + h_{21} \frac{dx}{dt} + h_{22} \frac{dy}{dt} + h_{23} \frac{dz}{dt} + x \left[ c_{21} + \chi_2 (1 - e^{-jT_v \omega}) (\rho + \rho \mu) + \sin(\varphi) h_3 \sigma t_p \alpha_2 \right] + \\ & + y \left[ c_{22} + \chi_2 (\rho + \rho \mu) S_p + \sin(\varphi) \sigma h_3 \right] + c_{23} z + Q \chi_2 \rho \mu \alpha_1 t_p S_p = 0, \\ & m \frac{d^2 z}{dt^2} + h_{31} \frac{dx}{dt} + h_{32} \frac{dy}{dt} + h_{33} \frac{dz}{dt} + x \left[ c_{31} + \chi_3 (1 - e^{-jT_v \omega}) (\rho + \rho \mu) + (k_{0t} + \Delta k_t) \sigma h_3 \alpha_2 t_p \right] + \\ & + y \left[ c_{32} + \chi_3 (\rho + \rho \mu) S_p + (k_{0t} + \Delta k_t) \sigma h_3 \right] + c_{33} z + Q \left[ \chi_3 \rho \mu \alpha_1 t_p S_p + \frac{\Delta k_t}{2} (\alpha_{f1} - \alpha_{f2}) t_p \sigma h_3 \right] = 0, \\ & (T_1 T_2) \frac{d^2 Q}{dt^2} + (T_1 + T_2) \frac{dQ}{dt} + \frac{dz}{dt} \left[ k_0 \chi_3 t_p S_p (\rho + \rho \mu) + k_0 (k_{0t} + \Delta k_t) \sigma h_3 t_p \right] + \\ & + \frac{dz}{dt} \left[ k_1 \chi_3 t_p S_p (\rho + \rho \mu) + k_1 (k_{0t} + \Delta k_t) \sigma h_3 t_p \right] e^{-jT_v \omega} + \\ & + x \left[ \chi_3 (1 - e^{-jT_v \omega}) (\rho + \rho \mu) V_c k_0 + (k_{0t} + \Delta k_t) \sigma h_3 \alpha_2 t_p V_c k_0 \right] + \\ & + x \left[ \chi_3 (1 - e^{-jT_v \omega}) (\rho + \rho \mu) V_c k_1 + (k_{0t} + \Delta k_t) \sigma h_3 \alpha_2 t_p V_c k_1 \right] e^{-jT_v \omega} + \\ & + y \left[ \chi_3 (\rho + \rho \mu) S_p k V_c + (k_{0t} + \Delta k_t) k V_c \sigma h_3 \right] + y \left[ \chi_3 (\rho + \rho \mu) S_p k_1 V_c + (k_{0t} + \Delta k_t) k_1 V_c \sigma h_3 \right] e^{-jT_v \omega} + \\ & + Q \left[ 1 + \chi_3 \rho \mu \alpha_1 t_p S_p k V_c + \frac{\Delta k_t}{2} (\alpha_{f1} - \alpha_{f2}) t_p \sigma h_3 k V_c \right] + \\ & + Q e^{-jT_v \omega} \left[ \chi_3 \rho \mu \alpha_1 t_p S_p k_1 V_c + \frac{\Delta k_t}{2} (\alpha_{f1} - \alpha_{f2}) t_p \sigma h_3 k_1 V_c \right] = 0, \end{aligned} \right. \quad (12)$$

The system (12)  $e^{-jT_v\omega}$  is like a lagging argument, where  $T_v$  is the revolution period of the workpiece. For the subsequent analysis of the control system, let's move on to the operator form of the system (12), it means, let's implement the *Laplace* transform, assuming that the initial conditions are zero ( $p = d/dt$ ), the following formulas are obtained.

$$\begin{cases}
 mp^2x(p) + h_{11}px(p) + h_{12}py(p) + h_{13}pz(p) + \\
 + x(p) \left[ c_{11} + \chi_1(1 - e^{-jT_v\omega})(\rho + \rho\mu) + \cos(\varphi)h_3\sigma t_p\alpha_2 \right] + \\
 + y(p) \left[ c_{12} + \chi_1(\rho + \rho\mu)S_p + \cos(\varphi)\sigma h_3 \right] + c_{13}z(p) + Q(p)\chi_1\rho\mu\alpha_1t_pS_p = 0, \\
 mp^2y(p) + h_{21}px(p) + h_{22}py(p) + h_{23}pz(p) + \\
 + x(p) \left[ c_{21} + \chi_2(1 - e^{-jT_v\omega})(\rho + \rho\mu) + \sin(\varphi)h_3\sigma t_p\alpha_2 \right] + \\
 + y(p) \left[ c_{22} + \chi_2(\rho + \rho\mu)S_p + \sin(\varphi)\sigma h_3 \right] + c_{23}z(p) + Q(p)\chi_2\rho\mu\alpha_1t_pS_p = 0, \\
 mp^2z(p) + h_{31}px(p) + h_{32}py(p) + h_{33}pz(p) + \\
 + x(p) \left[ c_{31} + \chi_3(1 - e^{-jT_v\omega})(\rho + \rho\mu) + (k_{0t} + \Delta k_t)\sigma h_3\alpha_2t_p \right] + \\
 + y(p) \left[ c_{32} + \chi_3(\rho + \rho\mu)S_p + (k_{0t} + \Delta k_t)\sigma h_3 \right] + c_{33}z(p) + \\
 Q(p) \left[ \chi_3\rho\mu\alpha_1t_pS_p + \frac{\Delta k_t}{2}(\alpha_{f1} - \alpha_{f2})t_p\sigma h_3 \right] = 0, \\
 (T_1T_2)p^2Q(p) + (T_1 + T_2)pQ(p) + pz(p) \left[ k_0\chi_3t_pS_p(\rho + \rho\mu) + k_0(k_{0t} + \Delta k_t)\sigma h_3t_p \right] + \\
 + pz(p) \left[ k_1\chi_3t_pS_p(\rho + \rho\mu) + k_1(k_{0t} + \Delta k_t)\sigma h_3t_p \right] e^{-jT_v\omega} + \\
 + x(p) \left[ \chi_3(1 - e^{-jT_v\omega})(\rho + \rho\mu)V_c k_0 + (k_{0t} + \Delta k_t)\sigma h_3\alpha_2t_pV_c k_0 \right] + \\
 + x(p) \left[ \chi_3(1 - e^{-jT_v\omega})(\rho + \rho\mu)V_c k_1 + (k_{0t} + \Delta k_t)\sigma h_3\alpha_2t_pV_c k_1 \right] e^{-jT_v\omega} + \\
 + y(p) \left[ \chi_3(\rho + \rho\mu)S_p k V_c + (k_{0t} + \Delta k_t)k V_c \sigma h_3 \right] + \\
 + y(p) \left[ \chi_3(\rho + \rho\mu)S_p k_1 V_c + (k_{0t} + \Delta k_t)k_1 V_c \sigma h_3 \right] e^{-jT_v\omega} + \\
 + Q(p) \left[ 1 + \chi_3\rho\mu\alpha_1t_pS_p k V_c + \frac{\Delta k_t}{2}(\alpha_{f1} - \alpha_{f2})t_p\sigma h_3 k V_c \right] + \\
 + Q(p)e^{-jT_v\omega} \left[ \chi_3\rho\mu\alpha_1t_pS_p k_1 V_c + \frac{\Delta k_t}{2}(\alpha_{f1} - \alpha_{f2})t_p\sigma h_3 k_1 V_c \right] = 0.
 \end{cases} \tag{13}$$

It is convenient to consider the system (13) in matrix-vector form:

$$\begin{pmatrix} a_{11} & a_{12} & a_{13} & a_{14} \\ a_{21} & a_{22} & a_{23} & a_{24} \\ a_{31} & a_{32} & a_{33} & a_{34} \\ a_{41} & a_{42} & a_{43} & a_{44} \end{pmatrix} \begin{pmatrix} x(p) \\ y(p) \\ z(p) \\ Q(p) \end{pmatrix} = 0, \tag{14}$$

where the coefficients have the following values:

$$\left\{ \begin{array}{l}
 a_{11} = mp^2 + h_{11}p + c_{11} + \chi_1(1 - e^{-jT_v\omega})(\rho + \rho\mu) + \cos(\varphi)h_3\sigma t_p\alpha_2, \\
 a_{12} = h_{12}p + c_{12} + \chi_1(\rho + \rho\mu)S_p + \cos(\varphi)\sigma h_3, \\
 a_{13} = h_{13}p + c_{13}, \\
 a_{14} = \chi_1\rho\mu\alpha_1 t_p S_p, \\
 a_{21} = h_{21}p + c_{21} + \chi_2(1 - e^{-jT_v\omega})(\rho + \rho\mu) + \sin(\varphi)h_3\sigma t_p\alpha_2, \\
 a_{22} = mp^2 + h_{22}p + c_{22} + \chi_2(\rho + \rho\mu)S_p + \sin(\varphi)\sigma h_3, \\
 a_{23} = h_{23}p + c_{23}, \\
 a_{24} = \chi_2\rho\mu\alpha_1 t_p S_p, \\
 a_{31} = h_{31}p + c_{31} + \chi_3(1 - e^{-jT_v\omega})(\rho + \rho\mu) + (k_{0t} + \Delta k_t)\sigma h_3\alpha_2 t_p, \\
 a_{32} = h_{32}p + c_{32} + \chi_3(\rho + \rho\mu)S_p + (k_{0t} + \Delta k_t)\sigma h_3, \\
 a_{33} = mp^2 + h_{33}p + c_{33}, \\
 a_{34} = \chi_3\rho\mu\alpha_1 t_p S_p + \frac{\Delta k_t}{2}(\alpha_{f1} - \alpha_{f2})t_p\sigma h_3, \\
 a_{41} = \chi_3(1 - e^{-jT_v\omega})(\rho + \rho\mu)V_c k_0 + (k_{0t} + \Delta k_t)\sigma h_3\alpha_2 t_p V_c k_0 + \\
 + \left[ \chi_3(1 - e^{-jT_v\omega})(\rho + \rho\mu)V_c k_1 + (k_{0t} + \Delta k_t)\sigma h_3\alpha_2 t_p V_c k_1 \right] e^{-jT_v\omega}, \\
 a_{42} = \chi_3(\rho + \rho\mu)S_p k_0 V_c + (k_{0t} + \Delta k_t)k_0 V_c \sigma h_3 + \\
 + \left[ \chi_3(\rho + \rho\mu)S_p k_1 V_c + (k_{0t} + \Delta k_t)k_1 V_c \sigma h_3 \right] e^{-jT_v\omega}, \\
 a_{43} = p \left[ k_0 \chi_3 t_p S_p (\rho + \rho\mu) + k_0 (k_{0t} + \Delta k_t) \sigma h_3 t_p \right] + \\
 + p \left[ k_1 \chi_3 t_p S_p (\rho + \rho\mu) + k_1 (k_{0t} + \Delta k_t) \sigma h_3 t_p \right] e^{-jT_v\omega}, \\
 a_{44} = (T_1 T_2) p^2 + (T_1 + T_2) p + \left[ 1 + \chi_3 \rho \mu \alpha_1 t_p S_p k_0 V_c + \frac{\Delta k_t}{2} (\alpha_{f1} - \alpha_{f2}) t_p \sigma h_3 k_0 V_c \right] + \\
 + e^{-jT_v\omega} \left[ \chi_3 \rho \mu \alpha_1 t_p S_p k_1 V_c + \frac{\Delta k_t}{2} (\alpha_{f1} - \alpha_{f2}) t_p \sigma h_3 k_1 V_c \right].
 \end{array} \right. \quad (15)$$

Subsequently, it is necessary to move to the time domain by replacing  $p = j\omega$ , and the characteristic polynomial of the control system is nothing more than the determinant of the matrix  $A$  presented in equation (14).

$$D(j\omega) = \det(A) = \begin{vmatrix} a_{11} & a_{12} & a_{13} & a_{14} \\ a_{21} & a_{22} & a_{23} & a_{24} \\ a_{31} & a_{32} & a_{33} & a_{34} \\ a_{41} & a_{42} & a_{43} & a_{44} \end{vmatrix}. \quad (16)$$

Thus, the equation (16) is the characteristic polynomial of the control system that needs to be researched for behavior on the complex plane when the frequency of  $\omega$  changes from zero to infinity.

## Simulation results and discussion of the first hypothesis

For the convenience of representing the behavior of the system, simulation was carried out in the *Matlab/Simulink 2014* package, where a nonlinear system (8), (10) was directly modeled in *Simulink*, and the characteristic polynomial (16) was calculated by a cycle in *Matlab* itself, where at every step of the cycle a determinant for a specific frequency value was considered, and the resulting value was deposited on the complex plane, then everything was repeated. In general, the value for  $\omega$  was calculated from zero to 2,000 Hz in increments of 0.01 Hz.

To assess the stability of the cutting control system by the *Mikhailov* method, the variants of the control system, the variant of a stable and the variant of an unstable (at the boundary of stability) system were considered. The factor affecting the stability of the cutting process was a tool wear along the flank; the second factor is the processing speed factor. Here there is a possibility of checking the *A.D. Makarov* statement. In total, 29 high-speed cutting modes were considered, in each of which a stable, unstable and at the boundary of stability cutting mode was studied.

Let's consider the set of parameters of the cutting control system, which includes a processing speed of 1,600 rpm and a wear value of 0.22 mm. The results of modeling the coordinates of the system state and the corresponding phase directions are presented in Figure 2.

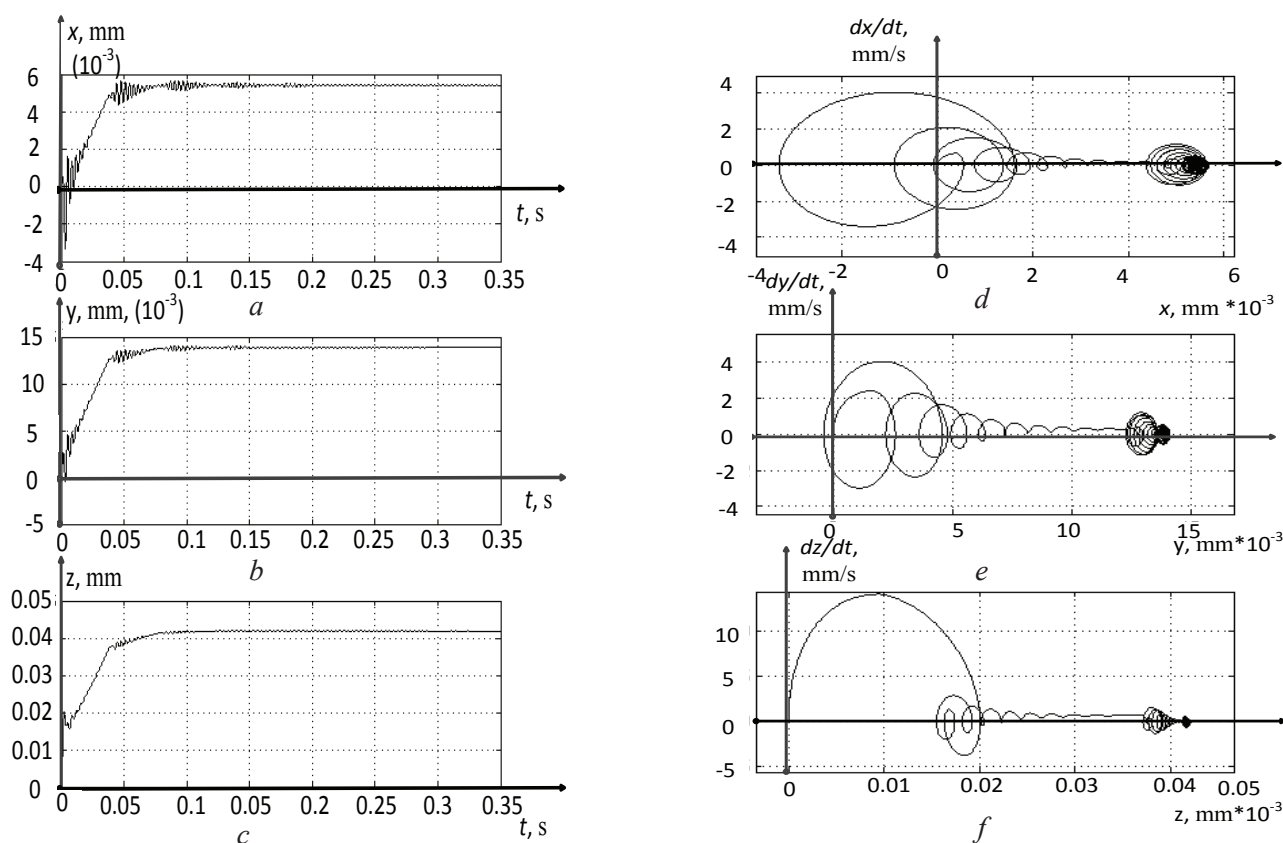


Fig. 2. For the case of wear  $h = 0.22$ :

*a* – deformations along the *x* coordinate; *b* – deformations along the *y* coordinate; *c* – deformations along the *z* coordinate; *d* – phase trajectory along the *x* coordinate; *e* – phase trajectory along the *y* coordinate; *f* – phase trajectory along the *z* coordinate

As can be seen from Figure 2, the system is stable, in addition, it can be seen from the phase trajectories that there is a constant restructuring of the control system, where the phase trajectory is compressed. However, each cycle of adjustment and subsequent compression is associated with cutting along the “trace” that was formed when the tool was embedded on the first turn.

The stability assessment according to the *Mikhailov* criterion, for the considered variant of the parameters of the cutting control system, is shown in Figure 3.

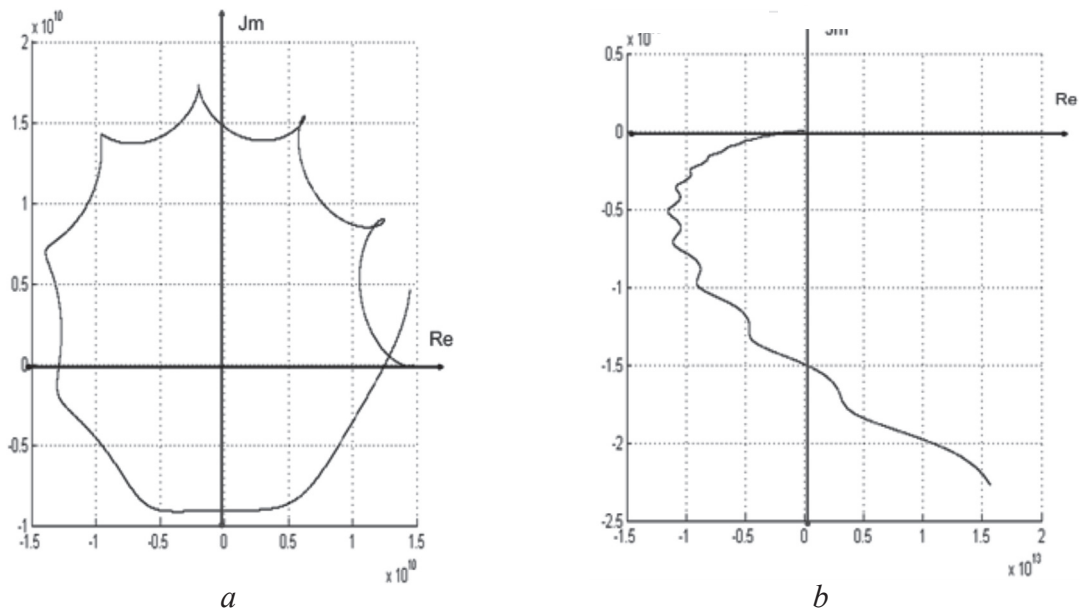


Fig. 3. The hodograph of the *Mikhailov* vector, a stable system:  
*a* – the beginning of the *Mikhailov* vector; *b* – the end of the *Mikhailov* vector

The *Mikhailov* vector hodograph, shown in Figure 3, confirms the conclusion about the stability of the cutting control system, which is made by analyzing the coordinates of the deformation motions of the tool tip earlier. A feature of the *Mikhailov* vector hodograph is a constant increase in the amplitude of the hodograph with the increase in the frequency of modeling, therefore, the description of the hodograph has to be done in two figures, in the first one we see the movement of the hodograph through the first five quadrants, and in the second the hodograph covers the point zero through three more quadrants.

The stability limit for the case of processing at a speed of 1,600 rpm, occurs at a wear value of 0.473 mm, the results of modeling the *Mikhailov* vector hodograph for this variant of modeling the cutting control system are shown in Figure 4.

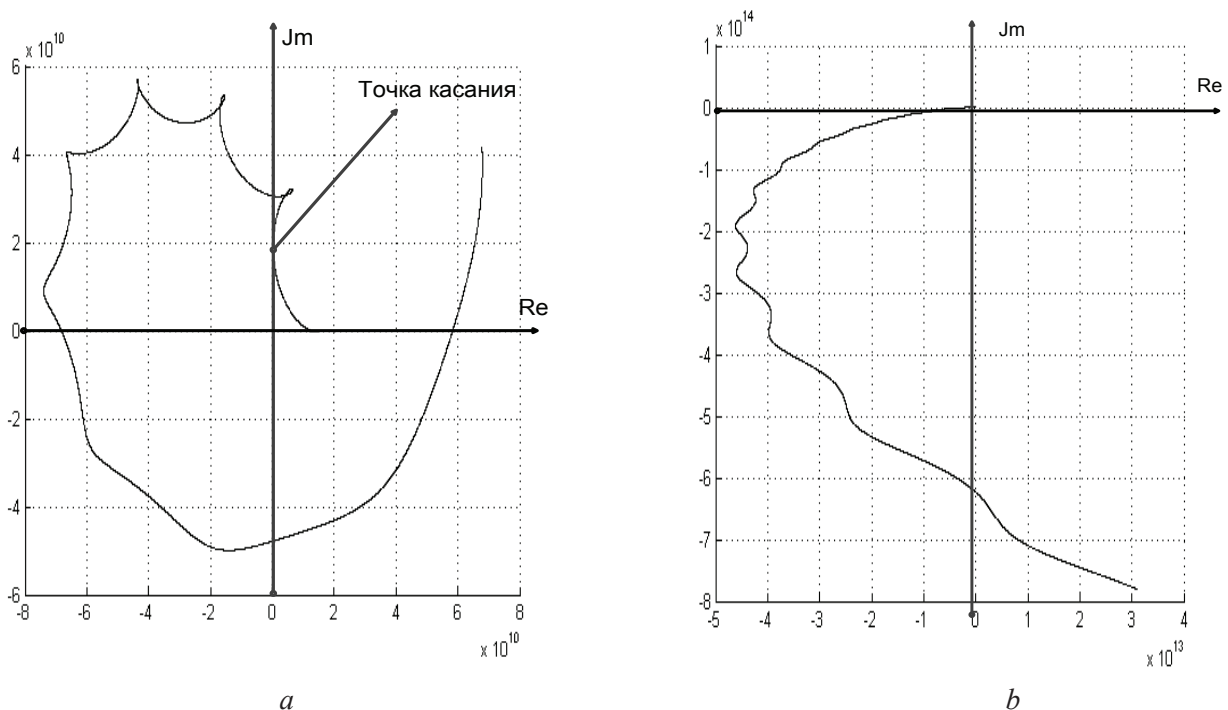


Fig. 4. The hodograph of the *Mikhailov* vector, the system on the boundary of stability:  
*a* – the beginning of the *Mikhailov* vector; *b* – the end of the *Mikhailov* vector

As it can be seen from Figure 4, the hodograph of the *Mikhailov* vector touches the imaginary axis and returns back to the first quarter, if this characteristic crosses the imaginary axis and returns back, it will be the mechanism for displaying the loss of stability of the system. Subsequently, with the increase in the amount of the cutting wedge wear, this is exactly what happens.

The results of all studies are summarized in one general table, which is given below.

Graphically, the area of stable dynamics of the cutting process, corresponding to the data given in Table 1, is shown in Figure 5.

Table 1

The boundary of the cutting system stability

$h_3$ , mm	0.3	0.32	0.34	0.35	0.37	0.38	0.4	0.41	0.42	0.43
$n$ , rev/m	300	340	400	440	500	600	660	700	760	820
$h_3$ , mm	0.436	0.44	0.445	0.4455	0.455	0.46	0.46	0.473	0.483	0.491
$n$ , rev/m	880	1,000	1,100	1,200	1,300	1,400	1,500	1,600	1,700	1,800

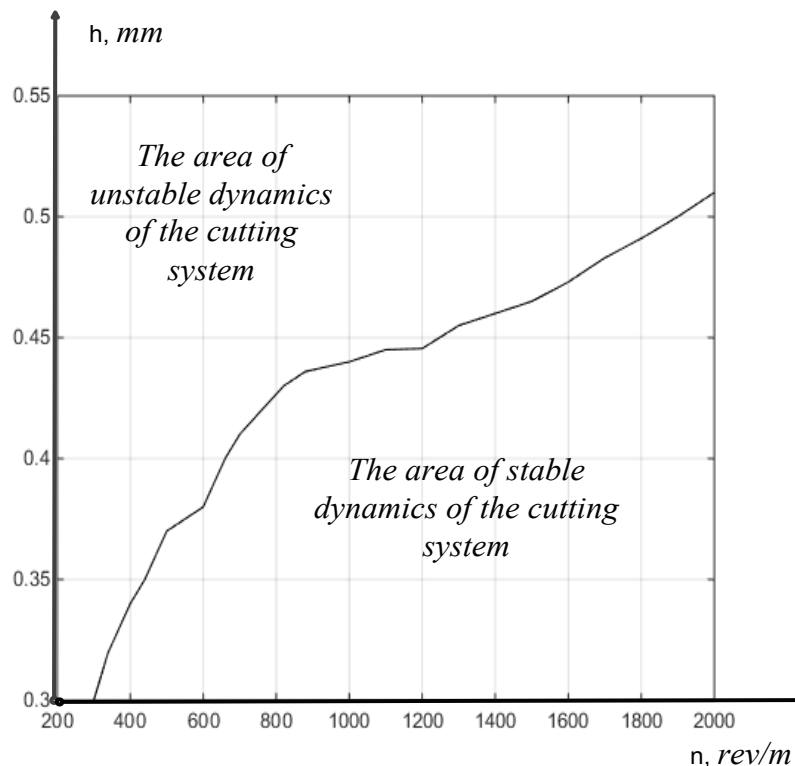


Fig. 5. Areas of stable and unstable behavior of the cutting system

As shown by Figure 5, the stability limit of the cutting system tends to grow indefinitely, while there is no pronounced maximum of this characteristic. In other words, the area of stable dynamics of the cutting system does not have a local extremum that would reflect the maximum dimensional stability of the tool corresponding to the statement, put forward by *A.D. Makarov*.

As the reason for such a strange behavior of the cutting control system, it can be indicated that the control system model given in this section does not actually include the structural adjustment of the force response, which is identified and described in [9]. To clarify this assumption, consider the variant of force responses at a cutting speed of 1,600 rpm, which are shown in Figure 6.

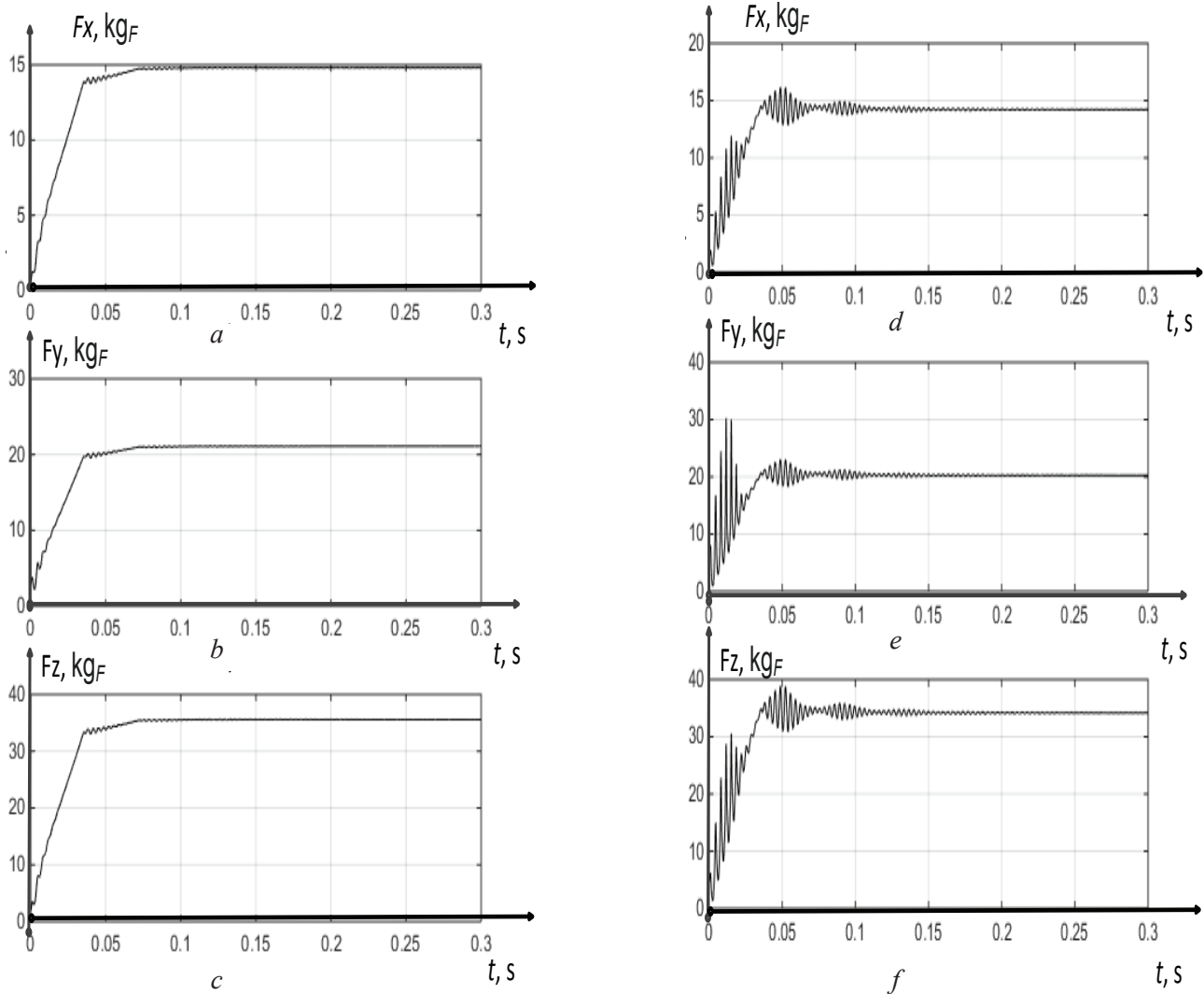


Fig. 6. Reaction forces for the option with a processing speed of 1,600 rpm:

$a - F_x$  for  $h = 0.22$ ;  $b - F_y$  for  $h = 0.22$ ;  $c - F_z$  for  $h = 0.22$ ;  $d - F_x$  for  $h = 0.49$ ;  $e - F_y$  for  $h = 0.49$ ;  $f - F_z$  for  $h = 0.49$

As it can be seen from Figure 6, despite a significant change in the wear of the cutting wedge along the flank, the stationary components of the response forces to the forming motions have hardly changed. It is also clear from the figure that the relations between these forces do not change either, which clearly contradicts the assumption about the restructuring of response forces.

Thus, the first hypothesis put forward at the beginning of the paper cannot be used as an objective for the scientific position put forward by *A.D. Makarov*. In other words, the combination of factors: the incident characteristic of the cutting force (according to *N.N. Zorev*) and the minimum coefficient of friction associated with the transition of friction from adhesive to diffusion nature is not sufficient to ensure the optimality of the cutting system according to the statement of *A.D. Makarov*. First of all, this is due to the lack of adjustment of the force response on the part of the cutting process to the forming motions of the tool with the increase in the wear of the cutting wedge along the flank.

## Testing the second hypothesis

### *Correction of the mathematical model of the cutting control system*

Let's consider the second statement put forward as an objective of the scientific position of *A.D. Makarov*, it is important to note that it is necessary to supplement the mathematical model describing the response of the cutting system to the forming motions of the tool with an additional element displaying the

dependence of the pushing force on the contact temperature of the tool and the workpiece. It is convenient to interpret this through the introduction of the dependence – the strength limit of the processed metal under compression on the corresponding contact temperature.

To determine this dependence, a series of experiments was carried out using the experimental setup *STD.201-1*, which involves adjusting the weighting coefficients to calculate the cutting temperature based on the values of the removed natural thermal *EMF*. The *STD.201-1* installation was developed by American engineers to solve the problems of analyzing the dynamics of cutting processes on machines of the turning group. The setup allows measuring the forces and vibrations of the tool, spread out along the axes of deformation (see Figure 1), as well as the temperature in the cutting zone. The research methodology provides for a whole setup procedure, which includes a double measurement of the contact temperature, a measurement using a natural thermal *EMF* and measurements carried out next to the contact with a calibrated thermocouple. An example of connection for the case of measuring the effect of contact temperature on the expulsive force, for the case of Steel 45, is shown in Figure 7.

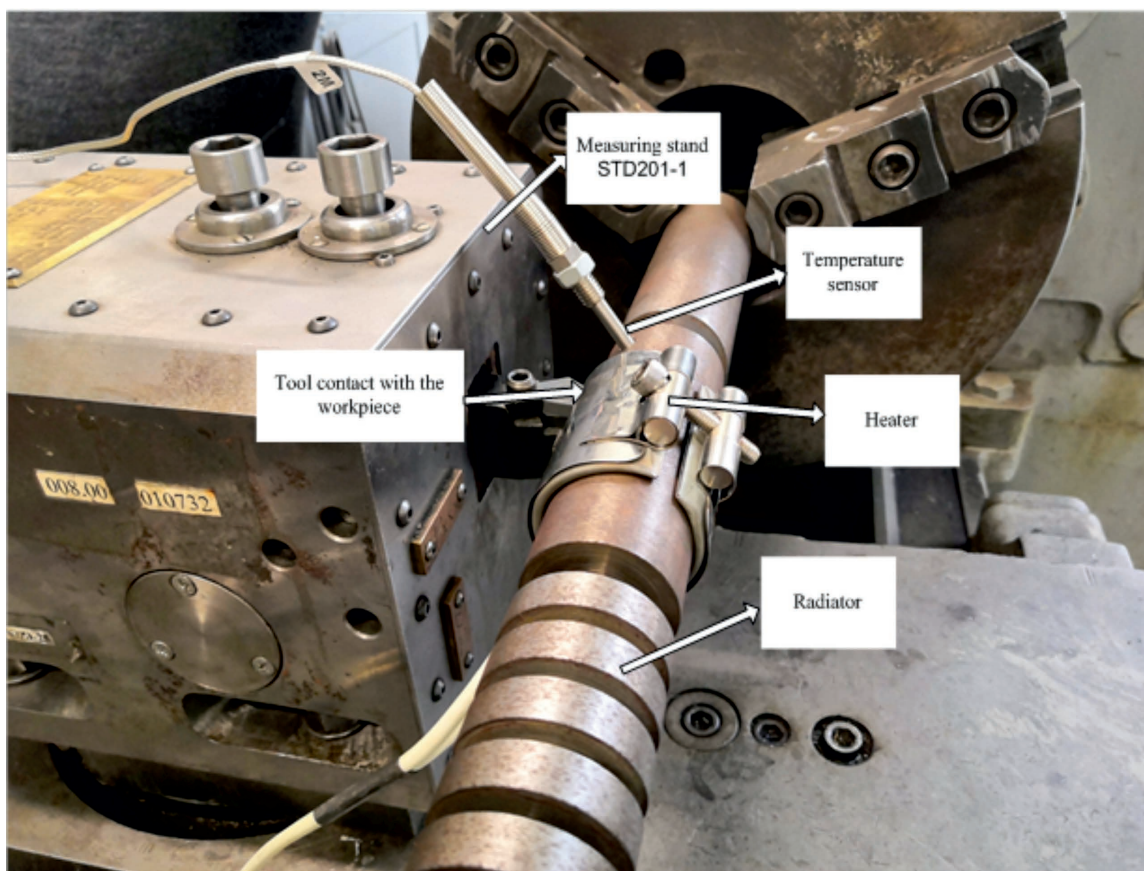


Fig. 7. Experimental setup prepared to assess the effect of contact temperature on the expulsive force

As can be seen from Figure 7, the measuring unit, in addition to the *STD201-1* stand, contains a specially prepared shaft made of Steel 45, which has a radiator working area, heated by a special circular heater that is put on the shaft. In addition, a tool is brought to the shaft with some effort, next to the contact, which has a thermocouple inserted into the shaft material that measures the real value of the contact temperature.

The measurement results are presented by the system's software interface, the appearance of which is shown in Figure 8.

As shown in Figure 8, the interface of the stand *STD201-1* provides for the possibility of the measuring subsystem calibration based on the measurement of the natural thermal *EMF* of the cutting zone. It was the calibration mode of this measuring stand that was used for the experiment to determine the dependence of the expulsive force on the contact temperature of the tool and the workpiece.

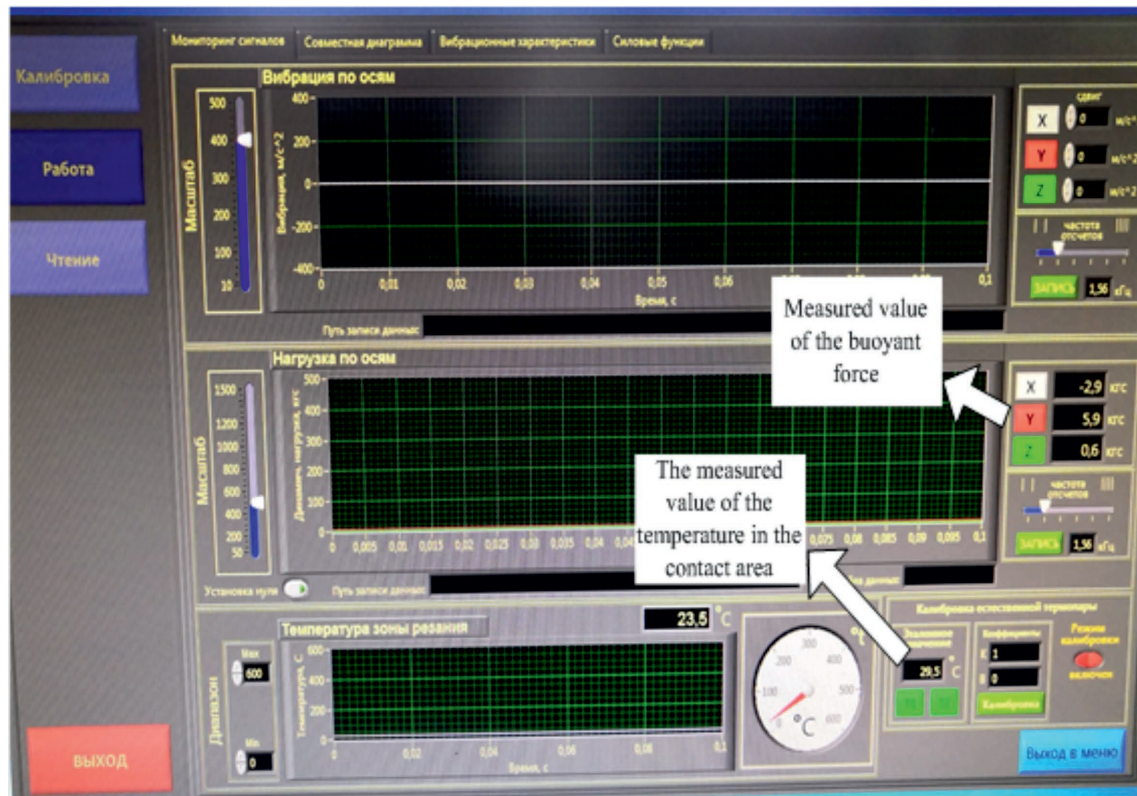


Fig. 8. Interface of the stand STD201-1

The results of experiments to assess the influence of the contact temperature on the value of the force pushing the tool out of the cutting zone, for the case of processing Steel 45, are shown in the table below (Table 2).

Table 2

**Dependence of  $F_y$  on the contact temperature**

$Q, ^\circ\text{C}$	30	40	50	60	70	80	90	100	110	120	130
$F_y, \text{kgF}$	9.5	9.7	10.3	10.9	11.5	12.2	12.8	13.4	13.8	14.3	14.6

A graphical representation of the experiment results is shown in Figure 9.

As is shown in Figure 9, the expulsive force almost linearly depends on the contact temperature, which is quite understandable from the point of view of the linear nature of metals expansion with the increase in its temperature. The average coefficient of linear increase in the expulsive force with the increase in the contact temperature  $k_Q^F$ , for the case of Steel 45, was 0.05625.

Thus, the experiments carried out showed that the expulsive force linearly depends on the temperature of the workpiece, for Steel 45 the coefficient of amplification of the expulsive force was 0.05625.

Let's imagine the dependence of the cutting force on the temperature-speed factor of cutting in the form of a falling exponential dependence of the coefficient  $\rho$  on the actual cutting speed, as it is presented in the figure below.

$$\rho = \rho_0 \left( 1 + \mu e^{-\alpha_1 \left( V_c - \frac{dz}{dt} \right)} \right), \quad (17)$$

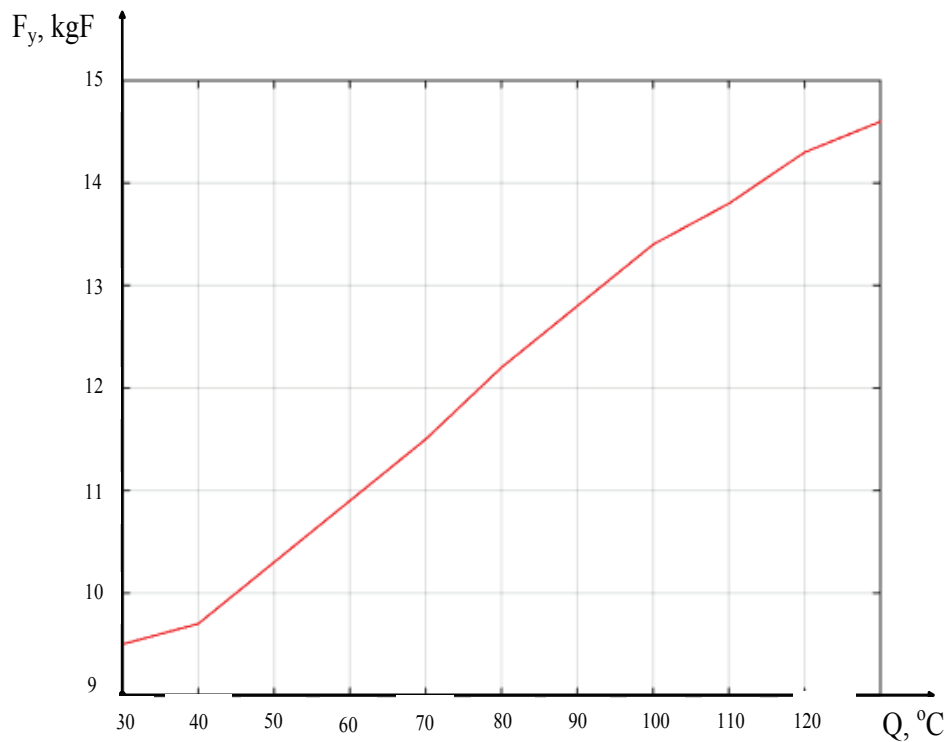


Fig. 9. Results of the experiment on Steel 45

where  $\rho_0$  – some minimum value of the coefficient  $\rho$ ;  $\mu$  – the coefficient showing the increase of the value  $\rho$  to some maximum value;  $\alpha_1$  – the steepness coefficient of the value drop  $\rho$ ;  $\left(V_c - \frac{dz}{dt}\right)$  – instantaneous cutting speed.

Taking into account expression (17), as well as relying on equation (1), the cutting force will be interpreted as:

$$F = \rho_0 \left(1 + \mu e^{-\alpha_1 \left(V_c - \frac{dz}{dt}\right)}\right) (t_p - y) \int_{t-T_v}^t \left(V_f - \frac{dx}{dt}\right) dt, \quad (18)$$

where  $(t_p - y)$  – instantaneous cutting depth,  $\int_{t-T_v}^t \left(V_f - \frac{dx}{dt}\right) dt$  – real feed.

Based on the feed transformation presented in the equation (18), we obtain the equation for calculating the feed in the following form:

$$\int_{t-T_v}^t \left(V_f - \frac{dx}{dt}\right) dt = V_f T_v - [x(t) - x(t - T_v)] = S_0 - x(1 - e^{-jT_v \omega}), \quad (19)$$

where  $S_0$  – the technological feed set by the CNC program, a  $x(1 - e^{-jT_v \omega})$  – the deformation motion of the cutting tool along the feed axis transformed through the delay link.

Equation (18), taking into account (19), will describe the cutting force, which after the linearization procedure in the vicinity of the equilibrium point, will take the following value:

$$\tilde{F} = -y \rho_0^{V_c} S_0 - x(1 - e^{-jT_v \omega}) \rho_0^{V_c} t_p + \frac{dz}{dt} \rho_0 \mu \alpha_1 t_p S_0, \quad (20)$$

where  $\rho_0^{V_c} = \rho_0 (1 + \mu(1 - \alpha_1 V_c))$ .

Let's consider, in the light of the conducted field experiments, the component of the force that depends on the wear of the tool along the flank, described in the previous section of the paper in the equation (2), which, taking into account the revealed linear dependence, can be conveniently considered as:

$$F_h = (\sigma_0 + k_Q^F Q_h) h_3 (t_p - y) e^{-K_h x}, \quad (21)$$

where  $\sigma_0$  – the ultimate strength of the processed metal under compression in  $[\text{kg}/\text{mm}^2]$ , at the contact temperature along the tool flank  $Q_h$  and the workpiece at zero degrees.

The linearized value of the force along the flank in the vicinity of the equilibrium point will have the following form:

$$\tilde{F}_h = -x K_h \sigma_0 h_3 t_p - y \sigma_0 h_3 + Q_h k_Q^h h_3 t_p. \quad (22)$$

In the description of the cutting force along  $z$  coordinate, there is a coefficient of friction described by the equation (5), a linearized version of this coefficient is given below:

$$k_t = k_{0t} + \Delta k_t (1 - K_{f1} Q_h) / 2 + \Delta k_t (1 + K_{f2} Q_h) / 2. \quad (23)$$

Taking into account (22 and (23), the linearized value  $F_h^{(z)}$  in the vicinity of the equilibrium point will take the form:

$$\begin{aligned} \tilde{F}_h^{(z)} = & -x K_h \sigma_0 h_3 t_p (k_{0t} + \Delta k_t) - y \sigma_0 h_3 (k_{0t} + \Delta k_t) + \\ & + Q_h \left[ k_Q^h h_3 t_p (k_{0t} + \Delta k_t) + (K_{f2} - K_{f1}) \Delta k_t \sigma_0 h_3 t_p \right]. \end{aligned} \quad (24)$$

The contact temperature of the tool flank and the workpiece is defined as the solution of the following differential equation:

$$T_1 T_2 \frac{d^2 Q_h}{dt^2} + (T_1 + T_2) \frac{d Q_h}{dt} + Q_h = k N (t - T), \quad (25)$$

where

$$N(t - T_v) = \left( \chi_3 F(t - T_v) + F_h^{(z)}(t - T_v) \right) \left( V_c - \frac{dz(t - T_v)}{dt} \right). \quad (26)$$

The equation (26) will take the form:

$$\begin{aligned} N(t - T_v) = & \chi_3 F(t - T_v) V_c + F_h^{(z)}(t - T_v) V_c - \\ & - \chi_3 F(t - T_v) \frac{dz(t - T_v)}{dt} - F_h^{(z)}(t - T_v) \frac{dz(t - T_v)}{dt}. \end{aligned} \quad (27)$$

The linearized value of irreversible transformations power in the vicinity of the equilibrium point will take the form:

$$\begin{aligned} N(t - T_v) = & -y \chi_3 e^{-j T_v \omega} \rho_0 V_c S_0 V_c - x \chi_3 (1 - e^{-j T_v \omega}) e^{-j T_v \omega} \rho_0 V_c t_p V_c + \frac{dz}{dt} e^{-j T_v \omega} \chi_3 \rho_0 \mu \alpha_1 t_p S_0 V_c - \\ & - x K_h \sigma_0 h_3 t_p (k_{0t} + \Delta k_t) e^{-j T_v \omega} V_c - y \sigma_0 h_3 (k_{0t} + \Delta k_t) e^{-j T_v \omega} V_c + \end{aligned}$$

$$\begin{aligned}
 &+Q_h \left[ k_Q^h h_3 t_p (k_{0t} + \Delta k_t) + (K_{f2} - K_{f1}) \Delta k_t \sigma_0 h_3 t_p \right] e^{-jT_v \omega} V_c - \\
 &\quad - \frac{dz}{dt} \left[ \chi_3 \rho_0 V_c S_0 + \sigma_0 h_3 t_p (k_{0t} + \Delta k_t) \right] e^{-jT_v \omega}.
 \end{aligned} \tag{28}$$

The general system of equations describing the dynamics of the cutting system is given below.

$$\left\{ \begin{aligned}
 &F = \rho_0 \left( 1 + \mu e^{-\alpha_1 \left( V_c - \frac{dz}{dt} \right)} \right) (t_p - y) \int_{t-T_v}^t \left( V_f - \frac{dx}{dt} \right) dt, \\
 &m \frac{d^2 x}{dt^2} + h_{11} \frac{dx}{dt} + h_{12} \frac{dy}{dt} + h_{13} \frac{dz}{dt} + c_{11} x + c_{12} y + c_{13} z = F_f, \\
 &m \frac{d^2 y}{dt^2} + h_{21} \frac{dx}{dt} + h_{22} \frac{dy}{dt} + h_{23} \frac{dz}{dt} + c_{21} x + c_{22} y + c_{23} z = F_p, \\
 &m \frac{d^2 z}{dt^2} + h_{31} \frac{dx}{dt} + h_{32} \frac{dy}{dt} + h_{33} \frac{dz}{dt} + c_{31} x + c_{32} y + c_{33} z = F_c, \\
 &F_f = \chi_1 F + F_h^{(x)}, \\
 &F_p = \chi_2 F + F_h^{(y)}, \\
 &F_c = \chi_3 F + F_h^{(z)}, \\
 &F_h = \left( \sigma_0 + k_Q^F Q_h \right) h_3 t_p e^{-K_h x}, \\
 &F_h^{(x)} = \cos \varphi F_h, \\
 &F_h^{(y)} = \sin \varphi F_h, \\
 &F_h^{(z)} = k_t F_h, \\
 &k_t = k_{0t} + \Delta k_t \left[ e^{-K_{f1} Q_z} + e^{K_{f2} Q_z} \right] / 2, \\
 &T_1 T_2 \frac{d^2 Q_h}{dt^2} + (T_1 + T_2) \frac{dQ_h}{dt} + Q_h = kN(t - T_v), \\
 &N(t - T_v) = \left( \chi_3 F(t - T_v) + F_h^{(z)}(t - T_v) \right) \left( V_c - \frac{dz(t - T_v)}{dt} \right).
 \end{aligned} \right. \tag{29}$$

The same system, but already in a linearized form, in the vicinity of the equilibrium point and after switching to the operator form of recording, will take the following form:

$$\left\{ \begin{aligned}
 &x(p) \left( mp^2 + h_{11}p + \chi_1(1 - e^{-jT_v\omega})\rho_0^V c t_p + \cos(\varphi)K_h\sigma_0 h_3 t_p + c_{11} \right) + \\
 &+ y(p) \left( h_{12}p + \chi_1\rho_0^V S_0 + \cos(\varphi)\sigma_0 h_3 + c_{12} \right) + \\
 &+ z(p) \left( h_{13}p - p\chi_1\rho_0\mu\alpha_1 t_p S_0 + c_{13} \right) - Q_h(p) \cos(\varphi)k_Q^h h_3 t_p = 0, \\
 &x(p) \left( h_{21}p + \chi_2(1 - e^{-jT_v\omega})\rho_0^V c t_p + \sin(\varphi)K_h\sigma_0 h_3 t_p + c_{21} \right) + \\
 &+ y(p) \left( mp^2 + h_{22}p + \chi_2\rho_0^V S_0 + \sin(\varphi)\sigma_0 h_3 + c_{22} \right) + \\
 &+ z(p) \left( h_{23}p - p\chi_2\rho_0\mu\alpha_1 t_p S_0 + c_{23} \right) - Q_h(p) \sin(\varphi)k_Q^h h_3 t_p = 0, \\
 &x(p) \left( h_{31}p + \chi_3(1 - e^{-jT_v\omega})\rho_0^V c t_p + c_{31} + K_h\sigma_0 h_3 t_p (k_{0t} + \Delta k_t) \right) + \\
 &+ y(p) \left( h_{32}p + \chi_3\rho_0^V S_0 + c_{32} + \sigma_0 h_3 (k_{0t} + \Delta k_t) \right) + z(p) \left( mp^2 + h_{33}p - p\chi_3\rho_0\mu\alpha_1 t_p S_0 + c_{23} \right) - \\
 &- Q_h(p) \left[ k_Q^h h_3 t_p (k_{0t} + \Delta k_t) + (K_{f2} - K_{f1})\Delta k_t \sigma_0 h_3 t_p \right] = 0, \\
 &x(p)k \left[ \chi_3(1 - e^{-jT_v\omega})e^{-jT_v\omega}\rho_0^V c t_p V_c + K_h\sigma_0 h_3 t_p (k_{0t} + \Delta k_t)e^{-jT_v\omega}V_c \right] + \\
 &+ y(p)k \left[ \chi_3 e^{-jT_v\omega}\rho_0^V S_0 V_c + \sigma_0 h_3 (k_{0t} + \Delta k_t)e^{-jT_v\omega}V_c \right] + \\
 &+ z(p)kp \left[ \left( \chi_3\rho_0^V S_0 + \sigma_0 h_3 t_p (k_{0t} + \Delta k_t) \right) e^{-jT_v\omega} - e^{-jT_v\omega}\chi_3\rho_0\mu\alpha_1 t_p S_0 V_c \right] + \\
 &+ Q_h(p) \left[ T_1 T_2 p^2 + (T_1 + T_2)p + 1 - \right. \\
 &\left. - k \left( k_Q^h h_3 t_p (k_{0t} + \Delta k_t) + (K_{f2} - K_{f1})\Delta k_t \sigma_0 h_3 t_p \right) e^{-jT_v\omega}V_c \right] = 0.
 \end{aligned} \right. \quad (30)$$

where  $p$  – the Laplace transform operator, which is equal to  $p = \frac{d}{dt}$  under zero initial conditions

The system (30) in matrix-vector form is given below:

$$\begin{cases}
 a_{11}(p)x(p) + a_{12}(p)y(p) + a_{13}(p)z(p) + a_{14}(p)Q_h(p) = 0, \\
 a_{21}(p)x(p) + a_{22}(p)y(p) + a_{23}(p)z(p) + a_{24}(p)Q_h(p) = 0, \\
 a_{31}(p)x(p) + a_{32}(p)y(p) + a_{33}(p)z(p) + a_{34}(p)Q_h(p) = 0, \\
 a_{41}(p)x(p) + a_{42}(p)y(p) + a_{43}(p)z(p) + a_{44}(p)Q_h(p) = 0.
 \end{cases} \quad (31)$$

where the coefficients of the matrix are:

$$A = \begin{pmatrix}
 a_{11}(p) & a_{12}(p) & a_{13}(p) & a_{14}(p) \\
 a_{21}(p) & a_{22}(p) & a_{23}(p) & a_{24}(p) \\
 a_{31}(p) & a_{32}(p) & a_{33}(p) & a_{34}(p) \\
 a_{41}(p) & a_{42}(p) & a_{43}(p) & a_{44}(p)
 \end{pmatrix}. \quad (32)$$

$a_{ij}$ ,  $i = 1 \dots 4, j = 1 \dots 4$ , are represented by the following expressions:

$$\left\{ \begin{array}{l}
 a_{11}(p) = mp^2 + h_{11}p + \chi_1(1 - e^{-jT_v\omega})\rho_0^V c t_p + \cos(\varphi)K_h\sigma_0 h_3 t_p + c_{11}, \\
 a_{12}(p) = h_{12}p + \chi_1\rho_0^V c S_0 + \cos(\varphi)\sigma_0 h_3 + c_{12}, \\
 a_{13}(p) = h_{13}p - p\chi_1\rho_0\mu\alpha_1 t_p S_0 + c_{13}), \\
 a_{14}(p) = \cos(\varphi)k_Q^h h_3 t_p, \\
 a_{21}(p) = h_{21}p + \chi_2(1 - e^{-jT_v\omega})\rho_0^V c t_p + \sin(\varphi)K_h\sigma_0 h_3 t_p + c_{21}, \\
 a_{22}(p) = mp^2 + h_{22}p + \chi_2\rho_0^V c S_0 + \sin(\varphi)\sigma_0 h_3 + c_{22}, \\
 a_{23}(p) = h_{23}p - p\chi_2\rho_0\mu\alpha_1 t_p S_0 + c_{23}, \\
 a_{24}(p) = \sin(\varphi)k_Q^h h_3 t_p, \\
 a_{31}(p) = h_{31}p + \chi_3(1 - e^{-jT_v\omega})\rho_0^V c t_p + c_{31} + K_h\sigma_0 h_3 t_p (k_{0t} + \Delta k_t), \\
 a_{32}(p) = h_{32}p + \chi_3\rho_0^V c S_0 + c_{32} + \sigma_0 h_3 (k_{0t} + \Delta k_t), \\
 a_{33}(p) = mp^2 + h_{33}p - p\chi_3\rho_0\mu\alpha_1 t_p S_0 + c_{23}, \\
 a_{34}(p) = k_Q^h h_3 t_p (k_{0t} + \Delta k_t) + (K_{f2} - K_{f1})\Delta k_t \sigma_0 h_3 t_p, \\
 a_{41}(p) = k \left[ \chi_3(1 - e^{-jT_v\omega})e^{-jT_v\omega}\rho_0^V c t_p V_c + K_h\sigma_0 h_3 t_p (k_{0t} + \Delta k_t)e^{-jT_v\omega}V_c \right], \\
 a_{42}(p) = k \left[ \chi_3 e^{-jT_v\omega}\rho_0^V c S_0 V_c + \sigma_0 h_3 (k_{0t} + \Delta k_t)e^{-jT_v\omega}V \right], \\
 a_{43}(p) = kp \left[ \left( \chi_3\rho_0^V c S_0 + \sigma_0 h_3 t_p (k_{0t} + \Delta k_t) \right) e^{-jT_v\omega} - e^{-jT_v\omega}\chi_3\rho_0\mu\alpha_1 t_p S_0 V_c \right], \\
 a_{44}(p) = T_1 T_2 p^2 + (T_1 + T_2)p + 1 - k \left( k_Q^h h_3 t_p (k_{0t} + \Delta k_t) + \right. \\
 \left. + (K_{f2} - K_{f1})\Delta k_t \sigma_0 h_3 t_p \right) e^{-jT_v\omega} V_c.
 \end{array} \right. \quad (33)$$

Similarly to the reasoning of the previous section, in the future it is necessary to move to the time domain by replacing  $p = j\omega$ , and the characteristic polynomial of the control system is nothing more than the determinant of the matrix  $A$ , what is seen in the following equation:

$$D(j\omega) = \det(A(j\omega)) = \begin{vmatrix} a_{11}(j\omega) & a_{12}(j\omega) & a_{13}(j\omega) & a_{14}(j\omega) \\ a_{21}(j\omega) & a_{22}(j\omega) & a_{23}(j\omega) & a_{24}(j\omega) \\ a_{31}(j\omega) & a_{32}(j\omega) & a_{33}(j\omega) & a_{34}(j\omega) \\ a_{41}(j\omega) & a_{42}(j\omega) & a_{43}(j\omega) & a_{44}(j\omega) \end{vmatrix}. \quad (34)$$

Thus, the expression (34) is a *Mikhailov* vector that should be followed for behavior on the complex plane when the frequency  $\omega$  changes from zero to infinity.

## Modeling results and discussion of the second hypothesis

For an adequate comparison of the experimental results in the previous section and the convenience of representing the system character, the simulation was carried out similarly to the previous version in the *Matlab/Simulink 2014* package, where the system (29) was directly modeled in *Simulink*; and the *Mikhailov* vector (34) was calculated by a cycle in *Matlab* itself, where at every step of the cycle the determinant  $D(j\omega)$  for a specific frequency value  $\omega$  was calculated and the resulting value was plotted along the complex plane, then everything was repeated. The simulation results for the case of processing with a cutting speed 900 rev/min are shown below.

Let's consider the dynamics of a nonlinear cutting system at a cutting speed 900 rev/min and  $h = 0.24$  mm, a graph of the coordinates of the deformation motion of the tool tip and the corresponding phase trajectories are shown in Figure 10.

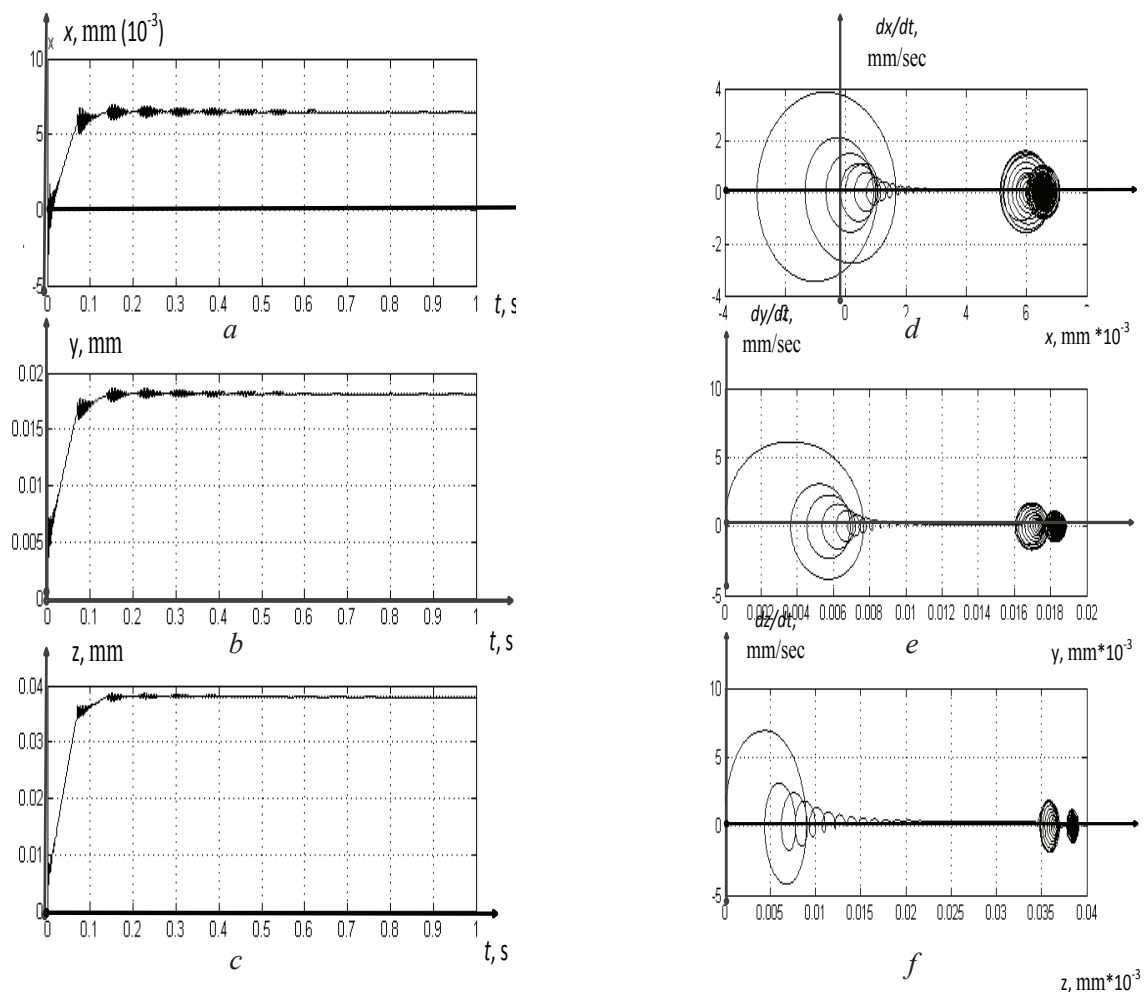


Fig. 10. For the case of wear  $h = 0.24$ :

*a* – deformations along the *x* coordinate; *b* – deformations along the *y* coordinate; *c* – deformations along the *z* coordinate; *d* – phase trajectory along the *x* coordinate; *e* – phase trajectory along the *y* coordinate; *f* – phase trajectory along the *z* coordinate

The dynamics of the cutting process reflected in Figure 10 shows a steady cutting process, which is associated with minimizing the vibration activity of the tool. The stability margin can be estimated from the starting point of the *Mikhailov* vector hodograph on the complex plane, which is shown in Figure 11.

As it can be seen from Figure 11, the stability margin depends on the distance of the hodograph curve beginning from the origin of the complex plane coordinates. The second part of the hodograph is not

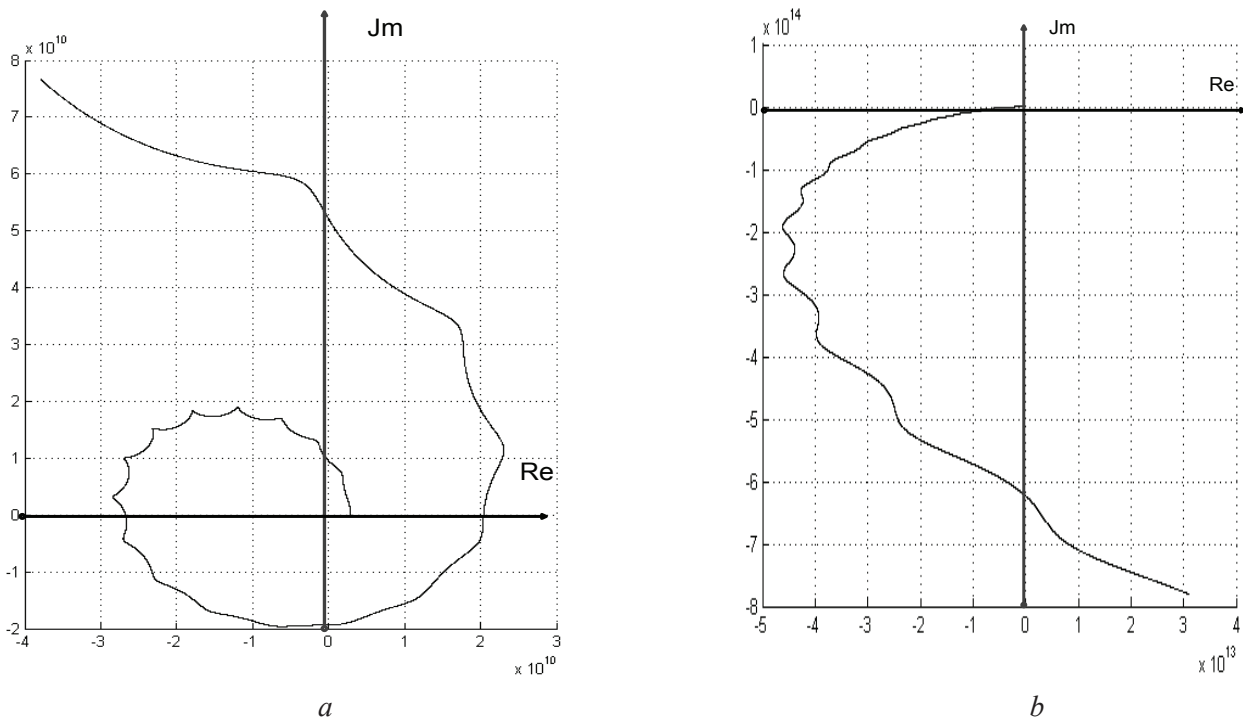


Fig. 11. The hodograph of the Mikhailov vector, a system with  $h = 0.24$ :  
 a – the beginning of the Mikhailov vector; b – the end of the Mikhailov vector

informative, as the loss of stability is displayed at the beginning of the hodograph; from these considerations, in the future, the second part (the end of the hodograph) will not be given.

Let's consider the analysis of the cutting control system stability at 0.36 mm wear, the results of modeling the Mikhailov vector hodograph are shown in Figure 12.

As shown by Figure 12, the beginning of the Mikhailov vector hodograph is still far from the origin of coordinates, but here the regenerative effect is clearly manifested, which in the linearized system of equations is described by the delay operator  $e^{-jT_s\omega}$ . The influence of this operator, in the initial section, becomes more significant with the increasing cutting speed, which leads to the increase in the fluctuations of the Mikhailov vector hodograph in the initial segment of the characteristic. As a result of such a change in the characteristics of the Mikhailov vector hodograph, the loss of stability may be associated with the entry of the Mikhailov vector hodograph into the second quadrant and subsequent return to the first quadrant. The point, where the hodograph is closest to the second quadrant (the convergence point on the graph) will determine the stability margin of the cutting system. As is clear from Figure 12, the hodograph of the Mikhailov vector leaves the first quadrant by cutting due to the influence of the delay operator on it. Let's consider this point more closely in Figure 12 on the right, from where it can be seen that the mechanism of reflection of the stability loss in the cutting system on the Mikhailov vector hodograph is associated with the intersection of the imaginary axis by the hodograph in the direction of the second quadrant of the complex plane. Such a change in the behavior of the hodograph is associated with the increase in the effect of the cutting system self-excitation, which in the English-language scientific literature, is commonly called the *regenerative effect*.

For the further analysis of the cutting control system, we will form into one table all the data obtained in previous parts of work on the upper limit of the stability of the cutting control system according to the Mikhailov criterion (see Table 3).

Table 3 shows that the maximum of the stability area of the cutting control system, in the space of the parameters of the cutting speed and the amount of the cutting wedge wear, is observed at a cutting speed of 1,620 rev/min. At this point, the amount of wear, allowed with regard to ensuring the stability of the machining process, was 0.47 mm, which is significantly higher than the average value for the sample, which was  $h \approx 0.39$  mm.

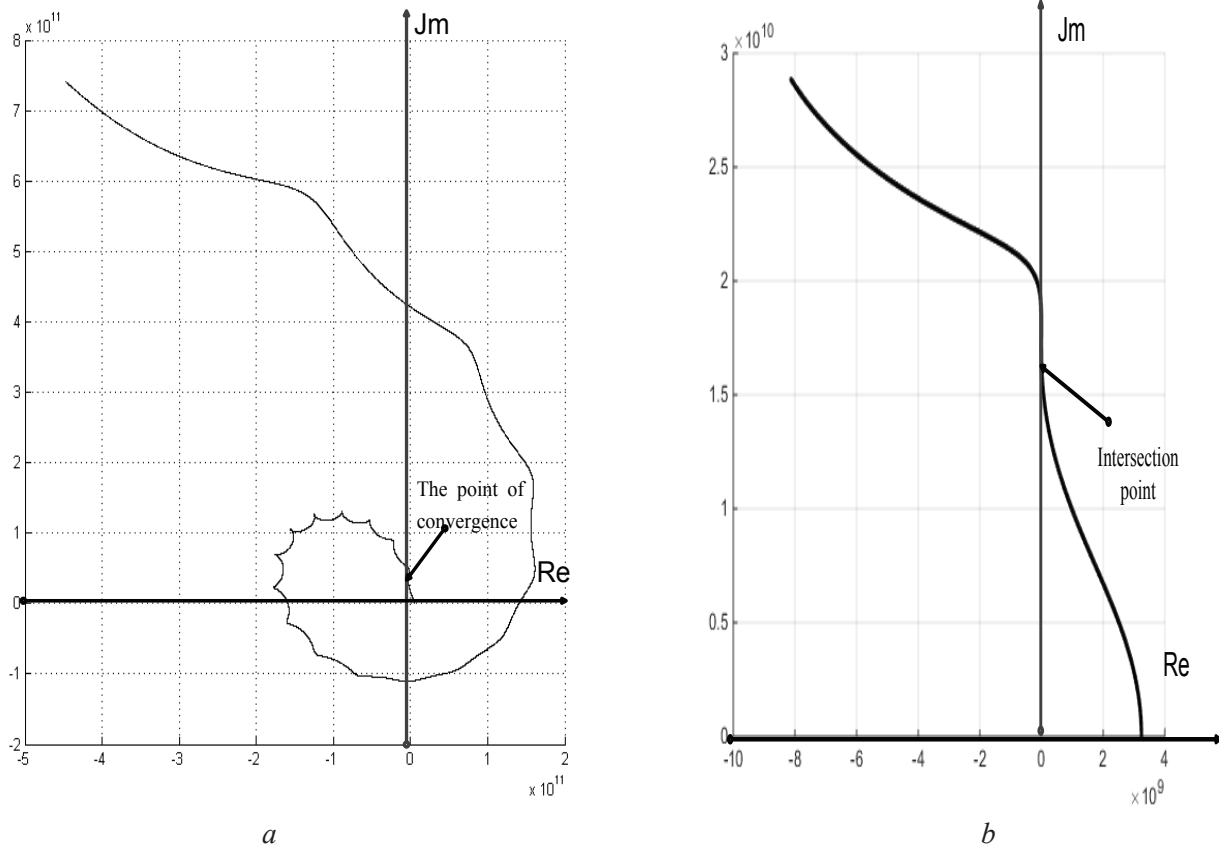


Fig. 12. The Mikhailov vector hodograph, a system with  $h = 0.36$ :

$a$  – the beginning of the Mikhailov vector;  $b$  – the enlarged beginning of the Mikhailov vector hodograph

Table 3

The boundary of the cutting system stability

$h_3$ (mm)	0.3	0.31	0.32	0.33	0.335	0.342	0.351	0.36	0.375	0.386
$n$ (rev/min)	360	460	660	760	820	900	1.000	1.100	1.200	1.300
$h_3$ (mm)	0.397	0.41	0.43	0.46	0.47	0.44	0.43	0.42	0.418	0.41
$n$ (rev/min)	1.400	1.500	1.560	1.600	1.620	1.680	1.700	1.750	1.800	1.900

Graphically, the interpretation of the data given in Table 3 is shown in Figure 13.

From Figure 13 it will be obvious that the area of stable dynamics of the cutting system definitely has a pronounced local maximum at a cutting speed of 1,620 rev/min. It should be noted that the studies conducted in the previous section did not give such a strong maximum (see Figure 5).

To verify the proposed assumption about the significant influence of the force response transformation from the cutting process on the forming motion of the tool, we consider the forces at the same processing speeds as in the previous case.

As it can be seen from Figure 14, with the increase in the wear of the cutting wedge of the tool, there is a significant restructuring of the force response of the cutting system, the  $F_x$  component increases by 5 %, the  $F_y$  component increases by 32 %, and  $F_z$  by 14 %.

Thus, the studies have shown that the increase in the pushing force, with the inevitable increase in the processing speed and the increase in the contact temperature, leads to a restructuring of the force response and a limitation of the stability area of the cutting system to the right of the local minimum.

Fig. 13. Areas of stable and unstable behavior of the cutting system

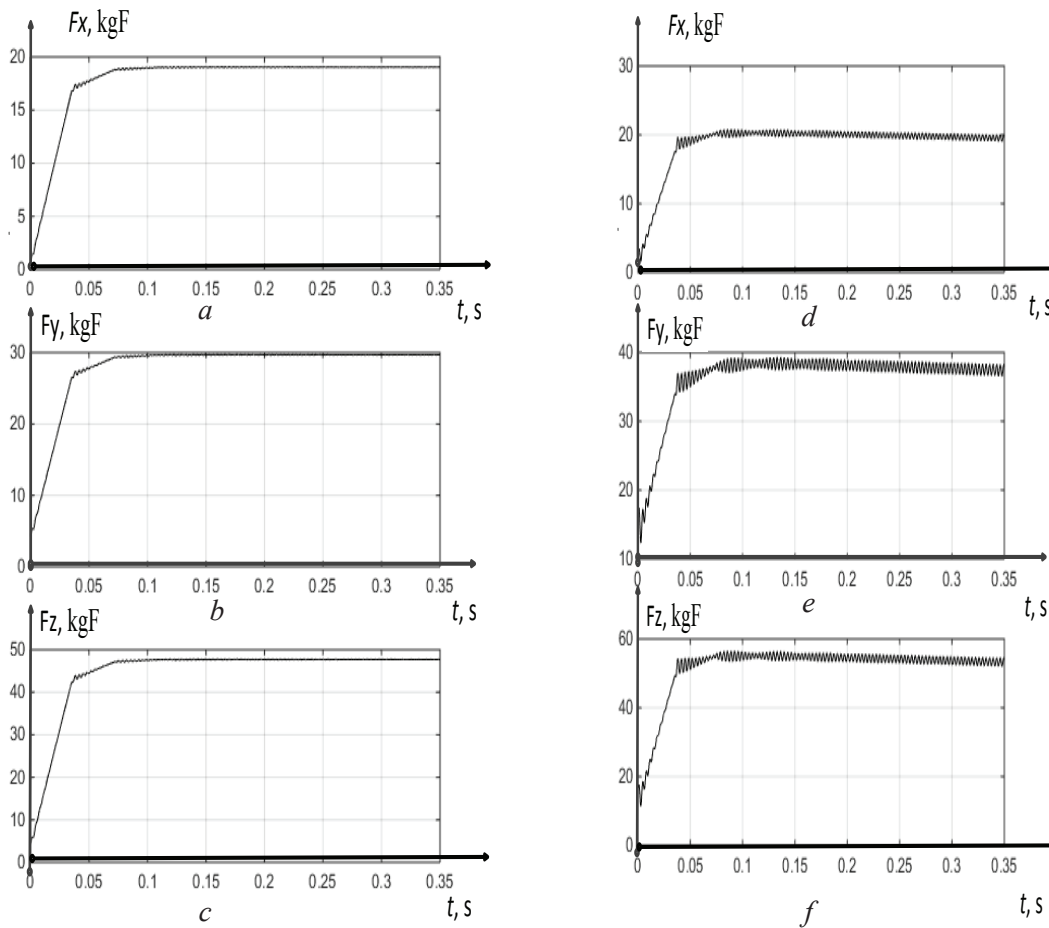
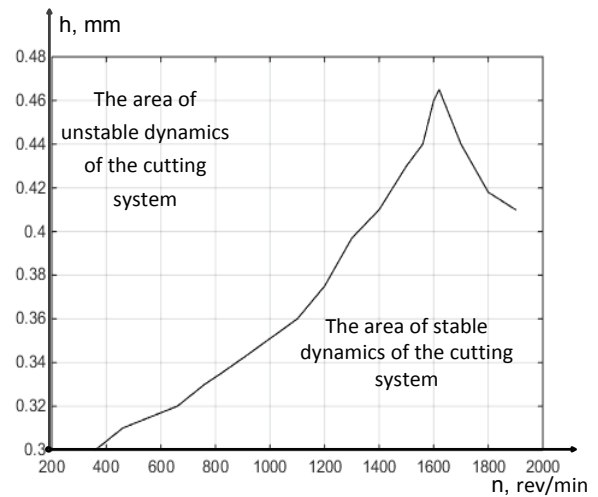


Fig. 14. Response forces for the option with a processing speed of 1,600 rpm:  
 a –  $F_x$  for  $h = 0.11$ ; b –  $F_y$  for  $h = 0.11$ ; c –  $F_z$  for  $h = 0.11$ ; d –  $F_x$  for  $h = 0.41$ ; e –  $F_y$  for  $h = 0.41$ ;  
 f –  $F_z$  for  $h = 0.41$

### Conclusions

The studies have shown that the first hypothesis put forward in the paper does not adequately reflect the position of *A.D. Makarov* about the existence of some optimal processing mode, but the second hypothesis generally confirms this position. Indeed, the optimal value of the cutting speed (cutting temperature), when modeling the dynamics of

the cutting process, is determined by a combination of the following factors: the incident characteristics of the cutting force (according to *N.N. Zorev*), the minimum coefficient of friction caused by the transition of friction from adhesive to diffusion nature and the dependence of the force pushing the tool from the preheated processing zone. However, it should be added here that another important factor determining the optimality of the cutting process according to *A.D. Makarov* is the regenerative effect inherent in the model of the cutting control system, which has a significant impact on the stability of the cutting system dynamics.

All this together allows us to formulate the following scientific position: the most optimal, with regard to a cutting speed (cutting temperature), will be the mode in which the incident characteristic of the cutting force (according to *N.N. Zorev*) reaches its minimum value, the coefficient of friction on the tool flank will be in the vicinity of the point of the local minimum, pushing the tool force will not exceed a certain pre-known value and, at the same time, the value of the cutting speed should be in the vicinity of a certain minimum of self-excitation of the cutting system during the regeneration of vibrations due to cutting along the “trace”.

From a practical point of view, the conducted research shows the possibility of introducing new measuring and computing subsystems that, based on a synthesized mathematical model, can determine the most optimal cutting modes in real time.

### References

1. Stépán G. Modelling nonlinear regenerative effects in metal cutting. *Philosophical Transactions of The Royal Society A: Mathematical Physical and Engineering Sciences*, 2001, vol. 359, pp. 739–757. DOI: 10.1098/rsta.2000.0753.
2. Litak G. Chaotic vibrations in a regenerative cutting process. *Chaos, Solitons and Fractals*, 2002, vol. 13, pp. 1531–1535. DOI: 10.1016/S0960-0779(01)00176-X.
3. Namachchivaya S., Beddini R. Spindle speed variation for the suppression of regenerative chatter. *Journal of Nonlinear Science*, 2003, vol. 13, pp. 265–288. DOI: 10.1007/s00332-003-0518-4.
4. Wahi P., Chatterjee A. Regenerative tool chatter near a codimension 2 Hopf point using multiple scales. *Nonlinear Dynamics*, 2005, vol. 40, iss. 4, pp. 323–338.
5. Stépán G., Insperger T., Szalai R. Delay, parametric excitation, and the nonlinear dynamics of cutting processes. *International Journal of Bifurcation and Chaos*, 2005, vol. 15, no. 09, pp. 2783–2798. DOI: 10.1142/S0218127405013642.
6. Moradi H., Bakhtiari-Nejad F., Movahhedy M.R., Ahmadian M.T. Nonlinear behaviour of the regenerative chatter in turning process with a worn tool: forced oscillation and stability analysis. *Mechanism and Machine Theory*, 2010, vol. 45, iss. 8, pp. 1050–1066. DOI: 10.1016/j.mechmachtheory.2010.03.014.
7. Gousskov A.M., Voronov S.A., Paris H., Batzer S.A. Nonlinear dynamics of a machining system with two interdependent delays. *Communications in Nonlinear Science and Numerical Simulation*, 2002, vol. 7, no. 4, pp. 207–221. DOI: 10.1016/S1007-5704(02)00014-X.
8. Lapshin V.P. Turning tool wear estimation based on the calculated parameter values of the thermodynamic subsystem of the cutting system. *Materials*, 2021, vol. 14, no. 21, p. 6492. DOI: 10.3390/ma14216492.
9. Lapshin V.P., Khristoforova V.V., Nosachev S.V. Vzaimosvyaz' temperatury i sily rezaniya s iznosom i vibratsiyami instrumenta pri tokarnoi obrabotke metallov [Relationship of temperature and cutting force with tool wear and vibration in metal turning]. *Obrabotka metallov (tekhnologiya, oborudovanie, instrumenty) = Metal Working and Material Science*, 2020, vol. 22, no. 3, pp. 44–58. DOI: 10.17212/1994-6309-2020-22.3-44-58.
10. Zakovorotny V.L., Gvindjiliya V.E. Evolution of the dynamic cutting system with irreversible energy transformation in the machining zone. *Russian Engineering Research*, 2019, vol. 39, no. 5, pp. 423–430. DOI: 10.3103/S1068798X19050204.
11. Zakovorotny V.L., Gvinjiliya V.E. Svyaz' prityagivayushchikh mnozhestv deformatsii instrumenta s prostanstvennoi orientatsiei uprugosti i regeneratsiei sil rezaniya pri tochenii [Correlation of attracting sets of tool deformations with spatial orientation of tool elasticity and regeneration of cutting forces in turning]. *Izvestiya vuzov. Prikladnaya nelineinaya dinamika = Izvestiya VUZ. Applied Nonlinear Dynamics*, 2022, vol. 30 (1), pp. 37–56. DOI: 10.18500/0869-6632-2022-30-1-37-56.
12. Zakovorotny V.L., Gvinjiliya V.E. Self-organization and evolution in dynamic friction systems. *Journal of Vibroengineering*, 2021, vol. 23, iss. 6, pp. 1418–1432. DOI: 10.21595/jve.2021.22033.



13. Astakhov V.P. The assessment of cutting tool wear. *International Journal of Machine Tools and Manufacture*, 2004, vol. 44, pp. 637–647. DOI: 10.1016/j.ijmachtools.2003.11.006.
14. Ryzhkin A.A. *Sinergetika iznashivaniya instrumental'nykh rezhushchikh materialov (triboelektricheskii aspekt)* [Synergetics of wear of tool cutting materials (triboelectric aspect)]. Rostov-on-Don, DSTU Publ., 2004. 323 p. ISBN 5-7890-0307-9.
15. Pereda J.A., Vielva L.A., Vegas A., Prieto A. Analyzing the stability of the FDTD technique by combining the von Neumann method with the Routh-Hurwitz criterion. *IEEE Transactions on Microwave Theory and Techniques*, 2001, vol. 49 (2), pp. 377–381.
16. Kolev L., Petrakieva S. Interval Raus criterion for stability analysis of linear systems with dependent coefficients in the characteristic polynomial. *27th International Spring Seminar on Electronics Technology: Meeting the Challenges of Electronics Technology Progress*. IEEE, 2004, vol. 1, pp. 130–135.
17. Zakovorotny V.L., Gvinjiliya V.E. Svyaz' samoorganizatsii dinamicheskoi sistemy rezaniya s iznashivaniem instrumenta [Link between the self-organization of dynamic cutting system and tool wear]. *Izvestiya vuzov. Prikladnaya nelineinaya dinamika = Izvestiya VUZ. Applied Nonlinear Dynamics*, 2020, vol. 28, no. 1, pp. 46–61. DOI: 10.18500/0869-6632-2020-28-1-46-61.
18. Velieva T.R., Kulyabov D.S., Korolkova A.V., Zaryadov I.S. The approach to investigation of the the regions of self-oscillations. *Journal of Physics: Conference Series*, 2017, vol. 937, p. 012057. DOI: 10.1088/1742-6596/937/1/012057.
19. Sourdille P., O'Dwyer A., Coyle E. Smith predictor structure stability analysis using Mikhailov stability criterion. *Proceedings of the 4th Wismarer Automatisierungs Symposium*, Wismar, Germany, 2005, pp. 22–23. DOI: 10.21427/kp1b-6034.
20. Saleh A.I., Hasan M.M.M., Darwish N.M.M. The Mikhailov stability criterion revisited. *JES. Journal of Engineering Sciences*, 2010, vol. 38, no. 1, pp. 195–207.
21. Barker L.K. *Mikhailov stability criterion for time-delayed systems*. Report NASA-TM-78803. NASA Langley Research Center, 1979. 17 p.
22. Makarov A.D. *Optimizatsiya protsessov rezaniya* [Optimization of cutting processes]. Moscow, Mashinostroenie Publ., 1976. 278 p.
23. Ryzhkin A.A., Shuchev K.G., Klimov M.M. *Obrabotka materialov rezaniem* [Processing of materials by cutting]. Rostov-on-Don, Feniks Publ., 2008. 418 p. ISBN 978-5-7890-0413-X.
24. Zorev N.N. *Voprosy mekhaniki protsessa rezaniya metallov* [Questions of mechanics of metal cutting process]. Moscow, Mashgiz Publ., 1956. 367 p.

## Conflicts of Interest

The authors declare no conflict of interest.

© 2023 The Authors. Published by Novosibirsk State Technical University. This is an open access article under the CC BY license (<http://creativecommons.org/licenses/by/4.0/>).

